Title
Channelized bottom melting and stability of floating ice shelves

Journal
Geophysical Research Letters, 35(2)

ISSN
0094-8276

Authors
Rignot, E
Steffen, K

Publication Date
2008

DOI
10.1029/2007gl031765

Channelized bottom melting and stability of floating ice shelves

E. Rignot[1,2] and K. Steffen[3]

Received 21 August 2007; revised 16 October 2007; accepted 23 November 2007; published 17 January 2008.

[1] The floating ice shelf in front of Petermann Glacier, in northwest Greenland, experiences massive bottom melting that removes 80% of its ice before calving into the Arctic Ocean. Detailed surveys of the ice shelf reveal the presence of 1–2 km wide, 200–400 m deep, sub-ice shelf channels, aligned with the flow direction and spaced by 5 km. We attribute their formation to the bottom melting of ice from warm ocean waters underneath. Drilling at the center of one of channel, only 8 m above sea level, confirms the presence of ice-shelf melt water in the channel. These deep incisions in ice-shelf thickness imply a vulnerability to mechanical break up and climate warming of ice shelves that has not been considered previously. **Citation:** Rignot, E., and K. Steffen (2008), Channelized bottom melting and stability of floating ice shelves, *Geophys. Res. Lett.*, *35*, L02503, doi:10.1029/2007GL031765.

1. Introduction

[2] Petermann Glacier, in northwestern Greenland, is one of the largest and most influential glaciers in north Greenland in terms of ice discharge into the ocean and drainage area [*Rignot et al.*, 2001]. It is also one of the few areas in Greenland where a significant portion of the drainage basin is grounded well below sea level [*Bamber et al.*, 2001], hence prone to rapid retreat if the glacier was pushed out of equilibrium by climate warming. Petermann Glacier flows from south to north into Petermann Fjord at about 1 km/yr and discharges ice into the Kennedy Channel, in the Arctic Ocean (Figure 1). It develops an extensive floating ice tongue, or ice shelf, 70 km in length and 20 km in width, the longest in the northern hemisphere. Remote sensing data collected in the 1990s indicate that pronounced bottom melting takes place underneath the ice shelf, and that its mass budget is dominated by ice-ocean interactions [*Rignot*, 1996]. The importance of bottom melting was shown to be common to ice shelves in north Greenland [*Rignot et al.*, 1997] and explains why iceberg production is low compared to grounding line fluxes [*Reeh et al.*, 1999].

[3] A field program was initiated in year 2002 to characterize the surface and bottom mass balances of the ice shelf in more details, compare the results with remote sensing estimates, deploy automated weather stations (AWS) to characterize local climate and surface energy balance, operate ground penetrating radar (GPR) to measure small-scale variations in ice thickness, measure ice velocity over a whole year using Geophysical Positioning System (GPS), and deploy a phase-sensitive radar system to measure bottom melting in situ [*Corr et al.*, 2002]. This paper focuses on the nature of ice-ocean interactions revealed by the survey, and the relevance of the results to the stability of ice shelves.

2. Data and Methodology

[4] Two AWS were deployed in year 2002 on the ice shelf to characterize local climate and measure the surface energy balance for model parameterization. Annual surface ablation was 1.2 m/yr of water between 2002 and 2005. Snow accumulation was negligible in 2002 and about 10 cm in 2003, 2004 and 2005, making it the driest region of the Greenland Ice Sheet [*Steffen and Box*, 2001].

[5] The glacier grounding line, where ice detaches from the bed and becomes afloat, was mapped with ERS-1/2 1-day repeat differential interferometric synthetic-aperture radar (InSAR) [*Rignot*, 1998]. Ice is 600 m thick at the grounding line. Ice thickness is from Kansas University's 150-MHz Ice Sounding Radar (ISR) [*Gogineni et al.*, 2001] with a vertical precision of 10 m. We also gathered higher resolution measurements using 50-MHz and 100-MHz GPR in years 2002, 2003 and 2004.

[6] Ice velocity was mapped using Radarsat-1 InSAR data with a 10-m/yr precision at 50-m posting. We detect no interannual variability in speed averaged over 24 days between year 2000 and 2006. In the summer, ice velocity increases by 8%. The latter is consistent with observations of other Greenland glaciers [*Rignot and Kanagaratnam*, 2006]. Petermann Glacier has had stable flow conditions over the past decade.

[7] We calculated the glacier ice discharge by combining vector velocity and ice thickness to obtain a flux of 12 ± 1 Gt/yt at the grounding line. For comparison, *Higgins* [1991] estimated iceberg production from this glacier to be 0.6 Gt/yr. Most of the difference in flux between the grounding line and the ice front is caused by removal of ice from the bottom by warm ocean waters.

[8] We calculated ice-shelf bottom melting from the divergence in ice discharge assuming steady state conditions, i.e. no change in ice thickness with time, negligible accumulation, and 1.2-m/yr surface melt. Area-average (10 km width × 6 km length) melt rates are plotted every 700 m in Figure 1. We did not use the entire glacier width (12 km) because ice thickness is not well constrained by observations along the margins. We bounded our averaging domain by two lines of ice thickness collected along flow lines so we could apply mass conservation in a simple fashion. Higher-resolution melt rates are shown in Figure 2. To obtain the latter, we smoothed the velocity field over 10 ice thicknesses (or 6 km) and calculated surface slopes and

[1]Earth System Science, University of California, Irvine, California, USA.
[2]Jet Propulsion Laboratory, Pasadena, California, USA.
[3]Cooperative Institute for Research in Environmental Sciences, University of Colorado, Boulder, Colorado, USA.

0094-8276/08/2007GL031765

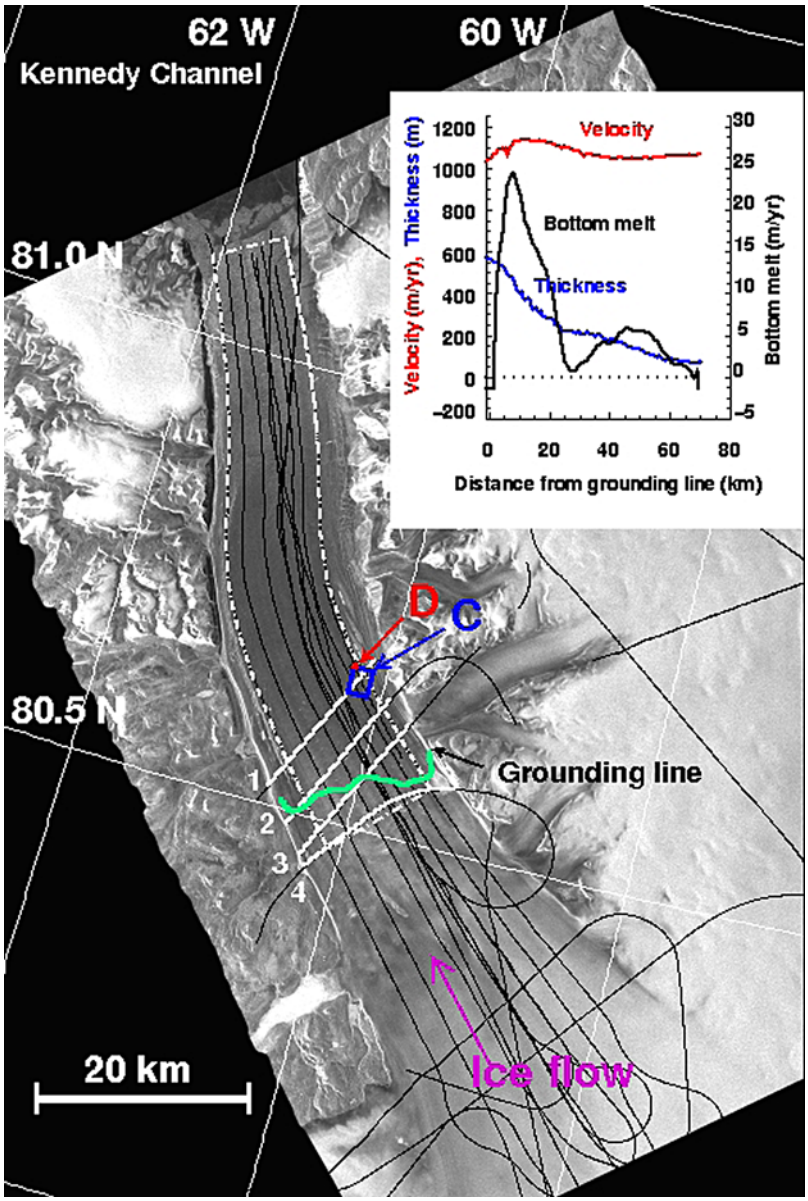

Figure 1. Radar brightness of Petermann Glacier from Radarsat-1, with laser/thickness aircraft survey flightlines (thin black lines), grounding line (thick green line), profiles 1–4 (white thick lines) of Figure 3, box C (blue) of Figure 4, and drilling site (red) D of Figure 5. Inset shows area-average bottom melting (10 km × 6 km) vs distance from grounding line calculated over the domain marked with white dotted lines.

strain rates over the same distance to deduce melt rates on a 600-m regular grid.

3. Results

[9] The area-average bottom melt rates (Figure 1) confirm earlier calculations made with sparser ice thickness data [*Rignot et al.*, 2001], and are consistent with the general pattern of ice-ocean interactions expected underneath an ice shelf [*Jenkins*, 1991]. Bottom melting increases from zero near the grounding line to peak at 25 m/yr about 10 km downstream, and subsequently decrease downstream. By the time the ice reaches the ice-shelf front, 80% of the thickness has been removed from the bottom, and 5% from surface melt.

[10] In the first 12 km (about one glacier width) of ice-shelf flow, we calculate an average melt rate of 18 m/yr. At 400 m depth, the melting point of seawater is depressed to −2.2°C, while the temperature of the ocean (discussed later) is +0.15°C. This yields a thermal forcing of the ocean of 2.35°C. The linear relationship of *Rignot and Jacobs* [2002] predicts an average melt rate of 23.5 m/yr, which is slightly higher than our estimate.

[11] The ISR data reveal pronounced spatial variations in ice thickness 1–2 km wide, 200–400 m deep, aligned with the flow direction and spaced by about 5 km (Figure 3). The channels are occasionally deeper than can be deduced from ice elevation data assuming hydrostatic equilibrium of the ice, e.g. at km 5 the ice is half as thick as required for hydrostatic equilibrium. The deepest channel, near km 5,

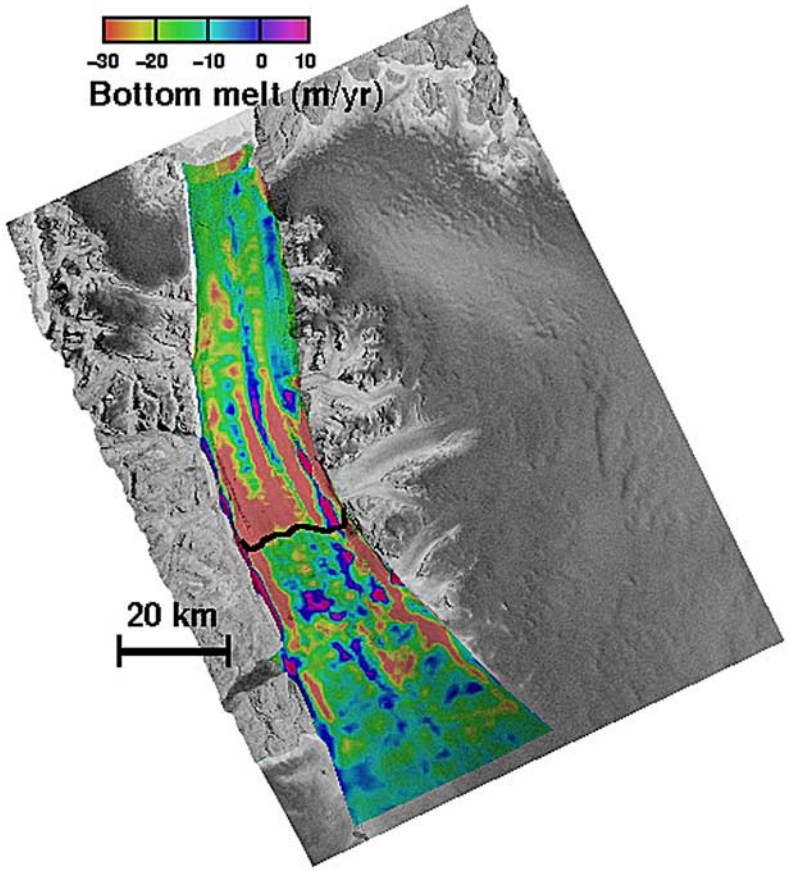

Figure 2. Petermann Glacier steady-state bottom melt rate in m/yr calculated on a 600-m grid from the divergence in ice flux. Values above the grounding line (thick black line) are affected by large errors due to sparse ice thickness data (Figure 1). On the ice shelf, ice thickness is better constrained by surface elevation data.

was mapped in details with GPR (Figure 4). The data show that the sub-ice-shelf channels have smooth, well-eroded sides with slopes away from vertical of 70°, i.e. that the channel opening angle is 140°.

[12] Detailed estimates of bottom melting (Figure 2) reveal a complex spatial pattern of high melting and ice deposition on the channel sides. The channels are aligned with the ice flow direction, and initially develop near the grounding line (Figure 3). Yet the channels have no surface or thickness expression on grounded ice that makes them distinguishable from the rest. We therefore attribute their formation entirely to the action of the ocean.

[13] The temperature/salinity profile of the ocean waters within the sub-ice-shelf channel (Figure 5) exhibits a linear relationship between 135 and 660 m depth, with a slope of 2.3°C per mil that is characteristic of the mixing of ice melt and seawater [*Gade*, 1979; *Potter and Paren*, 1985]. From 60 to 110 m depth, seawater is at its freezing point of −1.84°C, but does not get cooler than that. If refreezing were to take place at the top of the channel, we would observe an inflection point in the temperature profile, i.e. temperature would decrease when depth increases. Here, there is no frazil ice precipitation at the top of the channel.

[14] The temperature gradient, dT/dz, increases from 10^{-4} K/m at 65 m depth to 0.016 K/m at 135 m depth, and then decreases to 10^{-4} K/m at 600 m, near the ice shelf

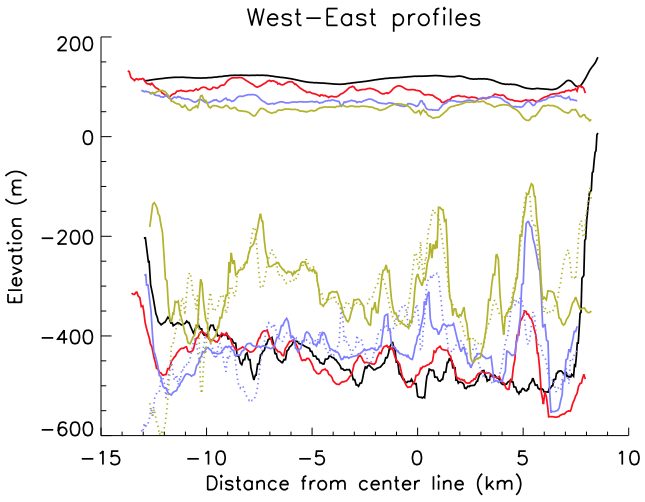

Figure 3. (top) Surface and (bottom) bed elevation of the ice shelf (continuous lines) and bed elevation deduced from hydrostatic equilibrium (dotted lines). Profiles 1–4 in Figure 1 are, resp., yellow, blue, red and black. Channels at km −8, −2, 1 and 5 deepen by 100 m's away from the grounding line.

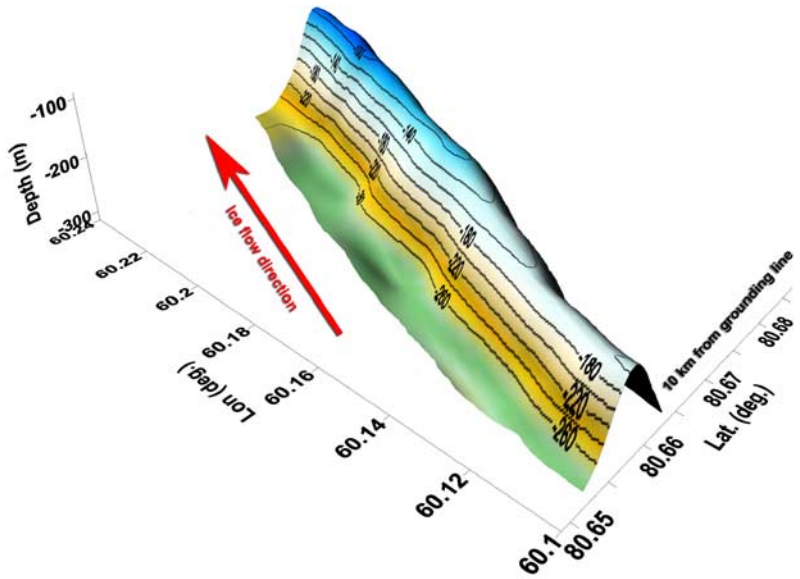

Figure 4. Three-dimensional view of the sub-ice-shelf melt channel near the field camp of Petermann Glacier (location C (blue) in Figure 1) obtained from ground penetrating radar (GPR). The melt channel deepens in the flow direction from −160 m to −80 m below the ice surface over a distance of 4.5 km.

draught. An analysis of these gradients assuming an eddy diffusion limited to vertical advection [*Potter and Paren*, 1985] suggests an upwelling of fresh-laden water along the sides of the channels, and a sinking of melt water down the center of the channel, as in the case of an ice-shelf rift [*Khazendar and Jenkins*, 2003]. Horizontal advection, however, is certainly significant in the present case since melt channels are oriented in the direction of ocean currents and of the main thermohaline circulation associated with ice-shelf melting. Ice-shelf rifts are, in contrast, usually oriented in a direction perpendicular to ocean currents and retain supercooled melt water at the top of the rift [*Khazendar and Jenkins*, 2003]. Here, buoyancy forces drive melt water along the lines of steepest slope to the center of the channel, and subsequently advect it downstream along the channel main axis. The convergence of less dense water to the channel center must increase the horizontal velocity of the mixed layer, which in turn increases the melt rate. This promotes channel growth in the vertical direction. Channel growth in the horizontal direction is driven by the pressure dependence of the melting point of seawater, which enhances melt along the deeper parts of the channels, as in the case of rifts.

4. Discussion

[15] The observation of large variations in bottom melting has important consequences. First, point measurements of bottom melting are difficult to extrapolate to large areas, regardless of their precision. Measurements taken at the center or a side of a channel may differ by orders of magnitudes [*Stewart et al.*, 2004]. Second, ice-shelf/ocean interfaces are not smooth, or with a fixed slope, but with undulations of several 100 m that affect the stratification of the water column, and in turn influence the melt regime of ice. Third, the surface of the channels is only a few meters above sea level (8.2 m in our case). Only a small increase in melting, from the surface or from below, would suffice to sever the ice shelf into large blocks. In the channel on the western side of the glacier, we saw seawater intruding through crevasses, illustrating that some channels are already sufficiently cracked to provide a direct pathway with the ocean waters underneath.

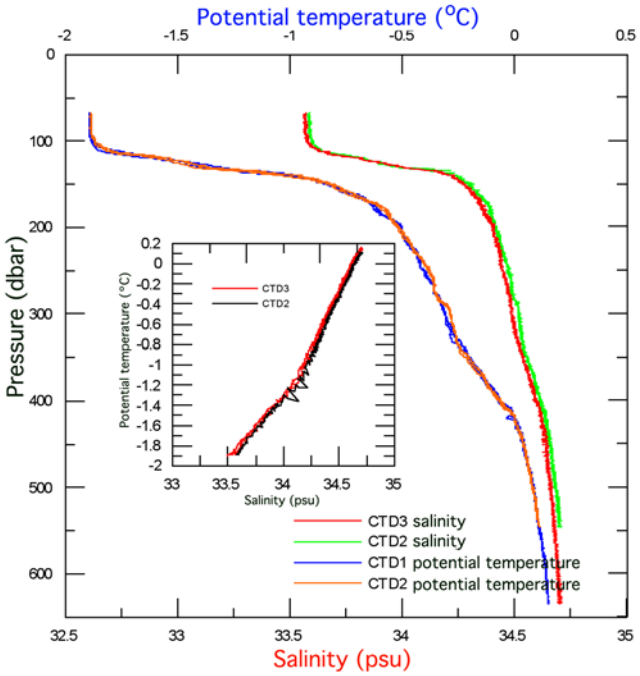

Figure 5. Potential temperature and salinity versus depth of sea water at the drilling site D in Figure 1. Inset shows potential temperature versus salinity. The top of the channel is at 60 dbar.

[16] If bottom melting increases in intensity, because the glacier is thicker or the ocean is warmer, the channels should get deeper. On Pine Island Glacier, Antarctica, melt rates exceed 50 m/yr near the grounding line, and sub-ice-shelf channels exhibit spatial variations in surface elevation that exceed 50 m [*Thomas et al.*, 2004] vs 20–25 m on Petermann Glacier. Conversely, channels at the mouth of ice streams flowing into the Ronne Ice Shelf are less deep than on Petermann Glacier, and bottom melting there is only in the range of a few m/yr [*Rignot and Jacobs*, 2002]. This suggests that melt channels are common to many ice shelves, but are only pronounced in areas of intense bottom melting.

5. Conclusions

[17] Ice-shelf bottom melting is confirmed by in-situ surveys to be the dominant component of the mass balance of the ice shelf in front of Petermann Glacier: it is 20 times larger than surface melting and 18 times larger than iceberg calving. This illustrates that ice-ocean interactions may exert a dominant control on the evolution of ice shelves in Greenland. These interactions are also highly spatially variable. They create sub-ice-shelf channels, regularly spaced across the glacier width, that deeply incise into the ice shelf bottom draft. In the case of Petermann Glacier, the channels are only a few 10 m's below the ice surface, whilst the ice shelf is 100 m's thick. If this pattern is common to many ice shelves, and for instance to those in Pine Island Bay, West Antarctica, it means that an increase in ice-shelf melting caused by warmer ocean waters will break up those ice shelves much sooner than would be predicted from the mean reduction in ice-shelf thickness.

[18] **Acknowledgments.** This work was performed at the Jet Propulsion Laboratory, California Institute of Technology, and at the University of Colorado in Boulder under a contract with the National Aeronautics and Space Administration's Cryospheric Science Program and with the National Science Foundation Office of Polar Program, Arctic Sciences. We thank the Swiss Federal Institute of Technology and M. Funk and A. Bader for the drill, Nick Cullen, Russel Huff, and Craig Stewart for their help in the field, W. Krabill and S. Gogineni for airborne data, A. Khazendar for discussion, and two anonymous reviewers for their comments. SAR data were provided by the European Space Agency and the Canadian Space Agency.

References

Bamber, J. L., R. L. Layberry, and S. P. Gogineni (2001), A new thickness and bed data set for the Greenland Ice Sheet: 1. Measurements, data reduction, and errors, *J. Geophys. Res.*, *106*, 33,773–33,780.

Corr, H. F. J., A. Jenkins, K. W. Nicholls, and C. S. M. Doake (2002), Precise measurement of changes in ice-shelf thickness by phase-sensitive radar to determine basal melt rates, *Geophys. Res. Lett.*, *29*(8), 1226, doi:10.1029/2001GL014606.

Gade, H. G. (1979), Melting of ice in sea water: A primitive model with application to the Antarctic Ice Shelf and icebergs, *J. Phys. Oceanogr.*, *9*, 189–198.

Gogineni, S., D. Tammana, D. Braaten, C. Leuschen, T. Akins, J. Legarsky, P. Kanagaratnam, J. Stiles, C. Allen, and K. Jezek (2001), Coherent radar ice thickness measurements over the Greenland Ice Sheet, *J. Geophys. Res.*, *106*, 33,761–33,772.

Higgins, A. (1991), North Greenland glacier velocities and calf ice production, *Polarforschung*, *60*, 1–23.

Jenkins, A. (1991), A one-dimensional model of ice shelf-ocean interaction, *J. Geophys. Res.*, *96*, 20,671–20,677.

Khazendar, A., and A. Jenkins (2003), A model of marine ice formation within Antarctic ice shelf rifts, *J. Geophys. Res.*, *108*(C7), 3235, doi:10.1029/2002JC001673.

Potter, J. R., and J. G. Paren (1985), Interaction between ice shelf and ocean in George VI Sound, Antarctica, in *Oceanology of the Antarctic Continental Shelf*, *Antarct. Res. Ser.*, vol. 43, edited by S. S. Jacobs, pp. 59–85, AGU, Washington, D. C.

Reeh, N., C. Mayer, H. Miller, H. Thomsen, and A. Weidick (1999), Present and past climate control on fjord glaciations in Greenland: Implications for IRD-deposition in the sea, *Geophys. Res. Lett.*, *26*, 1039–1042.

Rignot, E. (1996), Tidal flexure, ice velocities and ablation rates of Petermann Gletscher, Greenland, *J. Glaciol.*, *42*, 476–485.

Rignot, E. (1998), Hinge-line migration of Petermann Gletscher, north Greenland, detected using satellite radar interferometry, *J. Glaciol.*, *44*, 469–476.

Rignot, E., and S. Jacobs (2002), Rapid bottom melting widespread near Antarctic Ice Sheet grounding lines, *Science*, *296*, 2020–2023.

Rignot, E., and P. Kanagaratnam (2006), Changes in the velocity structure of the Greenland Ice Sheet, *Science*, *311*, 986–989.

Rignot, E., S. P. Gogineni, W. B. Krabill, and S. Ekholm (1997), Ice discharge from north and northeast Greenland as observed from satellite radar interferometry, *Science*, *276*, 934–937.

Rignot, E., W. Krabill, S. Gogineni, and I. Joughin (2001), Contribution to the glaciology of northern Greenland from satellite radar interferometry, *J. Geophys. Res.*, *106*, 34,007–34,020.

Steffen, K., and J. Box (2001), Surface climatology of the Greenland Ice Sheet: Greenland climate network 1995–1999, *J. Geophys. Res.*, *106*, 33,951–33,964.

Stewart, C., E. Rignot, K. Steffen, N. Cullen, and R. Ruff (2004), Basal topography and thinning rates of Petermann Gletscher, northern Greenland, measured by ground-based phase-sensitive radar, *FRISP Rep. 15*, Bjerknes Cent. for Clim. Res., Bergen, Norway.

Thomas, R., et al. (2004), Accelerated sea level rise from West Antarctica, *Science*, *306*, 255–258.

E. Rignot, Jet Propulsion Laboratory, 4800 Oak Grove Drive, MS 300-319, Pasadena, CA 91109-8099, USA. (erignot@uci.edu)

K. Steffen, CIRES, University of Colorado, Boulder, CO 80309, USA. (konrad.steffen@colorado.edu)